Hindawi
Geofluids
Volume 2022, Article ID 1007731, 10 pages
https://doi.org/10.1155/2022/1007731

Research Article

Analytical Method for Capped Pile–Soil Interaction considering the Load Action of Soil under the Pile Cap

Shilin Luo,[1,2] **Mingquan Liu**,[3] **Jianqing Jiang**,[1] **Ailifeila Aierken**,[1] **Jin Chang**,[1] **Xuewen Zhang**,[1] **and Rui Zhang**[1]

[1]*College of Civil Engineering, Changsha University, Changsha, Hunan 410022, China*
[2]*Guizhou Provincial Key Laboratory of Rock and Soil Mechanics and Engineering Safety, Guizhou University, Guiyang, Guizhou 550025, China*
[3]*School of Civil Engineering, Tangshan University, Tangshan, Hebei 063000, China*

Correspondence should be addressed to Mingquan Liu; lmq_1009@tsc.edu.cn

Received 8 November 2021; Revised 12 January 2022; Accepted 22 February 2022; Published 24 March 2022

Academic Editor: Mohammed Fattah

To study the pile–soil interaction mechanism of capped pile, an analytical method considering the load action of soil under the pile cap is proposed. The shearing displacement method is used to derive the lateral friction of pile body under the pile top load, and the Boussinesq solutions is used to derive the lateral friction of pile body considering the load of soil under the cap. The theoretical expressions of axial force and load-settlement curves are also achieved by means of establishing and solving the equilibrium differential equation of the pile body. Comparison of calculation results with the ordinary pile indicates that soil load under the pile cap reduces the lateral friction value; the influenced depth is about four times of the load action radius. The axial force and the load-settlement curve data are verified by a case history data. The results show that the computed data agree well with the measured data. The proposed method can direct the design of capped pile composite foundations.

1. Introduction

Capped pile is a type of reinforcement body in foundation; it is formed by placing a certain size of pile cap on the top of an ordinary pile body. The pile body is usually a prestressed pipe pile or solid concrete pile. The pile cap is normally a round or a square concrete slab. Capped piles have been widely used in soft soil treatment [1–3]. The original purpose of setting a cap on the pile top is to reduce the pile top penetration into the upper cushion and regulate the load sharing ratio of the pile and soil [4, 5]. With the increasing engineering applications, pile caps are found to raise the bearing capacity of piles and influence the working behavior of composite foundations, which many scholars have further researched [6–10]. The research methods include field test [11], model test [12–16], experiment test [17–19], and numerical simulation approaches [20–29].

When the pile settled under a vertical load, there is a displacement difference between the pile body and soil of the ordinary pile, while there is no such displacement difference between pile body and soil of capped pile due to the coordination of the cap. This leads to the pile body–soil interaction difference between capped pile and ordinary pile. Shang et al. analyzed the interaction of a flexible subsoil matrix and a piled box (raft) using Geddes stress factor [30]. The results show that the method is reliable. Cui et al. studied the response of pile groups in layered soil under the assumption that pile–cap–soil interaction is linear elastic [31]. The study used the shearing displacement method, and computed load-settlement curves were consistent but beneath the measured ones. Jin-bo and Cong-xin analyzed pile–soil interaction with a stiffness matrix method based on differential displacement of pile and soil. The pile lateral friction and pile tip load were assumed to be proportional to the respective displacement [32]. Wang et al. assumed that the distribution of skin friction on capped pile is simplified as two force triangles; by combining Mindlin-Geddes and Boussinesq solutions, the equation of the additional side stresses

for a single capped pile foundation is derived [33]. Chen et al. used a slider displacement method to consider the overall bearing capacity of capped piles. In their study, the Plandel shear slip failure model is used in the upper foundation soil bearing capacity analysis, and the load transfer method is used to analyze the bearing capacity of the lower pile body. This method is suitable for short, rigid piles with large pile caps under the condition of smooth soil interface with the pile cap [34].

To sum up, the pile–soil interaction is often considered in the settlement calculation of composite foundation. Compared with the large number of engineering applications, theoretical researches of capped pile–soil interaction are not extensive.

In this paper, we propose an analytical method to further study the pile–soil interaction mechanisms of capped piles with consideration to the load action of soil under the cap. Upper load is transmitted to the pile body and the soil under the cap through pile cap. The lateral frictional resistance of the capped body is superposed by friction caused by the load on the pile body and the load on the soil under the pile cap. By establishing the differential equilibrium equation of the pile body, the theoretical expressions of pile axial force and the load-settlement curve are deduced. The feasibility of this method is verified by comparing computed results with other methods and field test data of a case history. We anticipate that the present research could help to better understand the pile–soil interaction mechanism issues of capped pile, such as the relationship of load-settlement curves and treatment of soft soil foundation, and then provide some practical experience and enlightenment on the studying of the pile engineering.

2. Analysis Method of Pile–Soil Interaction

2.1. Analysis Model. When a vertical load is acting on the top of a pile cap, the load is transmitted downward by the pile cap. Because the pile cap is directly in contact with the pile body and the soil, the upper load is transferred to the pile body and the soil under the cap simultaneously. Due to the differential resistance stiffness of the pile body and the soil, each of them supports a different amount of load. Existing test results and finite element simulation results had confirmed that the load sharing phenomenon occurs throughout the pile body settlement process. The influence of the load on the soil under the pile cap cannot be ignored when analyzing the pile–soil interaction. To appropriately simplify the analysis, the following assumptions are used: (1) the pile cap is rigid and without bending and shearing deformation, (2) the pile body is rigid and without radial deformation, (3) the load transmitted to the pile top is equivalent to a concentrated load, and the load transmitted to the soil under the cap is equivalent to a uniformly distributed load, (4) the stress in foundation soil is calculated according to the elastic theory, and (5) the pile tip stress is calculated using the Winkler foundation model.

The mechanical model of a pile with cap is established, as shown in Figure 1, where R and r are the radii of the pile cap and pile body, respectively, q and q_1 are uniform loads acting on the pile top and soil under the cap, respectively, and P_t is the equivalent concentrated load acting on the pile top. The relationship among the variables is described:

$$P_t + q_1 \times \pi(R-r)^2 = q \times \pi R^2. \tag{1}$$

According to Figure 1 and assumption (3), a pile–soil interaction analysis model (Figure 2) is established on the above basis, where P_b is equivalent concentrated load at the pile tip and q_b is uniform load at the bottom of the soil under the cap.

When a concentrated load P_t is acted on the pile body alone, the lateral friction will appear on the pile side. When a uniform load q_1 is acted on the soil under cap individually, there will also be friction on the pile side. When they act together, the above two states can be superimposed. Then, the lateral friction on the pile–soil interface can be calculated by the superposition of τ_p and τ_q, which are derived from the concentrated load P_t acting on the top of the pile and the uniform load q_1 acting on the top of the soil under the cap, respectively.

2.2. Solution for Lateral Friction. First, we study the case of concentrated load P_t acting on the top of a pile. Rondoloph and Worth assumed that when a concentrated load is acting on a single pile, the soil around the pile only produces annular shear displacement, which can be approximately treated as a plane problem [35]. Thus, a rectangular coordinate system is employed to establish the calculation schematic diagram (Figure 3), and the origin of the coordinate axis is located at the pile body center.

According to the shearing displacement method, if l is the pile length, A_p is the area of the cross section of the pile body, U_p is the pile perimeter, E_p is the elastic modulus of the pile body, G_s is the shearing deformation modulus of the soil, ν is the Poisson ratio of the soil, ω_b is displacement of the pile tip, and r_m is the maximum influence radius that can be assigned as $0.5(1-\nu)l$, the expressions for lateral frictional resistance of the pile body $\tau_p(z)$, displacement of the pile body $\omega_p(z)$, axial force of the pile body $N_p(z)$, and equivalent concentrated load at the pile tip P_b are shown, respectively, as follows:

$$\tau_p(z) = \frac{k_1}{U_p}\omega_p(z), \tag{2}$$

$$\omega_p(z) = \omega_b \cos h[\lambda(l-z)], \tag{3}$$

$$N_p(z) = P_b\left\{\frac{k_1}{k_2}\sinh[\lambda(l-z)] + \cosh[\lambda(l-z)]\right\}, \tag{4}$$

$$P_b = k_{2\omega b}, \tag{5}$$

where λ^2 is the quotient of k_1 and A_pE_p and k_1 is the shear stiffness between the pile and soil, calculated as follows:

$$k\_1 = 2\pi G_s \ln^{-1}(r\_m/r). \tag{6}$$

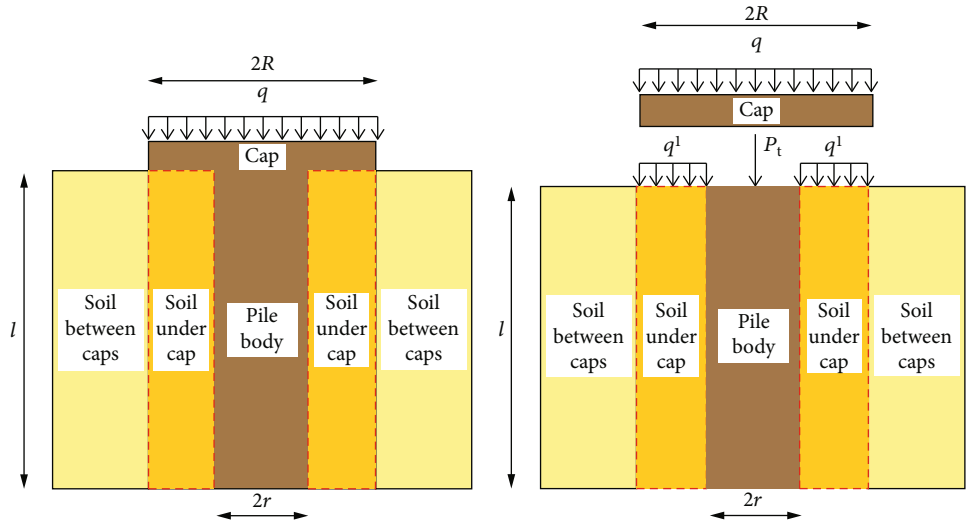

Figure 1: Mechanical model of capped pile.

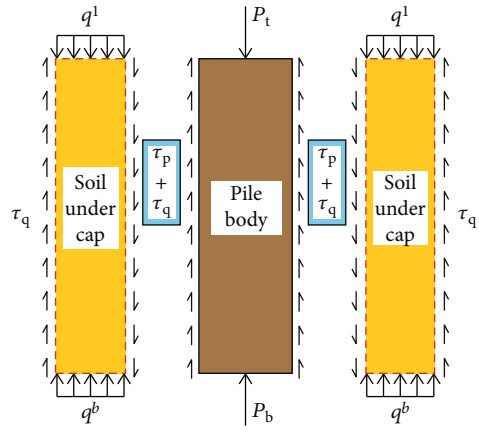

Figure 2: Pile–soil interaction analysis model.

The compressive stiffness of soil (k_2) beneath the pile tip can be calculated as follows:

$$k_2 = 4rG_s/(1-\upsilon). \tag{7}$$

Then, we study the case of uniform load q_1 acting on the soil under the cap. The same coordinate system is employed to establish the calculation schematic diagram (Figure 4). The pile–soil interface is located on the vertical plane with distance from the origin r; q_1 is effective in the range between r and R, and the coordinates of an arbitrary point P underground on the pile–soil interface are (r, z). The load on the micro unit dx is replaced by linear load $q_1 dx\,(r \le x \le R)$.

According to the plane stress solution [36], the additional shear stress $\tau_q(z)$ induced by linear load q_1 at point P at depth z $(0 \le z \le l)$ on the pile–soil interface is

$$\tau_q(z) = \frac{q_1}{\pi}\sin^2\theta, \tag{8}$$

where θ is the angle between the connection line of point P to unit dx and the pile–soil interface $(0 \le \theta \le \pi/2)$.

Substituting the geometrical relations in Figure 4(b) into Equation (8) produces

$$\tau_q(z) = \frac{q_1}{\pi}\frac{(R-r)^2}{z^2+(R-r)^2}. \tag{9}$$

Finally, the lateral friction on the pile–soil interface $\tau(z)$ is the sum of $\tau_p(z)$ and $\tau_q(z)$:

$$\tau(z) = \tau_p(z) + \tau_q(z). \tag{10}$$

Considering the directions of $\tau_p(z)$ and $\tau_q(z)$ produces

$$\tau(z) = \frac{k_1}{U_p}\cosh\left[\lambda(l-z)\right]\cdot\omega_b - \frac{q_1}{\pi}\cdot\frac{(R-r)^2}{z^2+(R-r)^2}. \tag{11}$$

2.3. Solutions for Axial Force and Settlement. When the expression of lateral friction is obtained, take the pile body in Figure 2 as a calculation isolator (Figure 5).

According to the force balance of the pile body, the equilibrium equation is established:

$$N(z) = P_t - \int_0^z U_p\tau(z)dz = P_t - \int_0^z U_p\left(\tau_p(z)+\tau_q(z)\right)dz. \tag{12}$$

By solving the integral, the axial force expression $N(z)$ is obtained:

$$N(z) = N_p(z) + 2rq_1\left[(R-r) - z\arctan\frac{R-r}{z}\right], \tag{13}$$

where $N_p(z)$ is the axial force of an ordinary pile body.

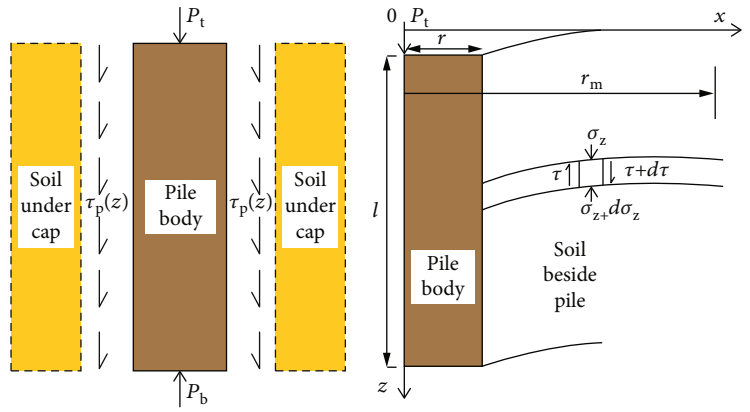

(a) Load schematic (b) Calculation schematic [35]

Figure 3: Calculation schematic diagram of P_t.

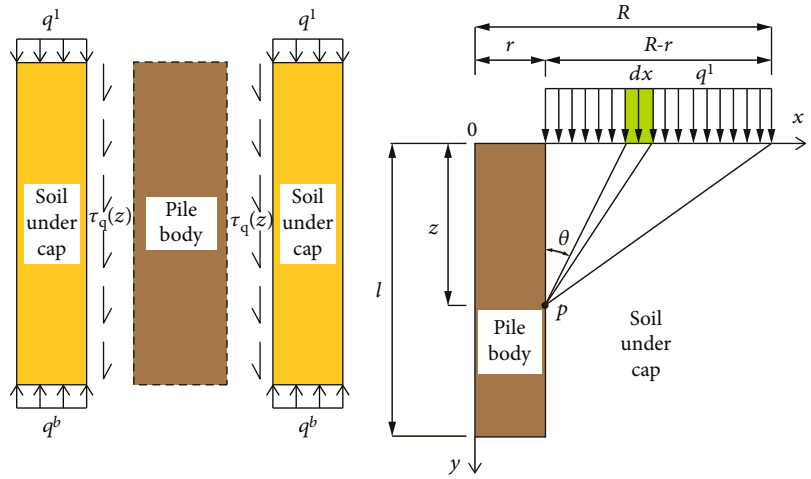

(a) Load schematic (b) Calculation schematic

Figure 4: Calculation schematic of soil load q_1.

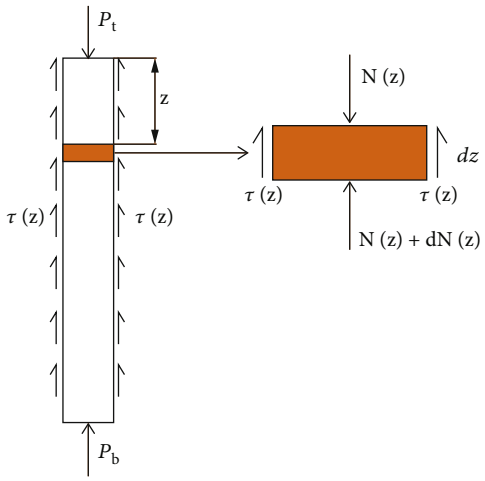

Figure 5: Calculation isolator.

According to the elastic compression conditions of a pile body, the relationship of displacement and frictional resistance of the pile side is expressed as Equation (14), and the relationship of axial force and displacement of the pile body is expressed as

$$\omega(z) = \frac{1}{A_p E_p} \int_l^z U_p \cdot \tau(z) dz, \tag{14}$$

$$N(z) = A_p E_p \cdot \frac{dw(z)}{dz}. \tag{15}$$

By substituting Equations (2), (3), and (9) into Equation (10), the lateral friction of the capped pile is obtained as

$$\tau(z) = \frac{P_t \cdot k_2 \cdot \cosh\left[\lambda(l-z)\right]}{U_p \cdot \left[k_1 \cdot \sinh\left(\lambda l\right) + k_2 \cdot \cosh\left(\lambda l\right)\right]} - \frac{q_1 \cdot (R-r)^2}{\pi \cdot \left[z^2 + (R-r)^2\right]}. \tag{16}$$

By substituting Equation (11) into Equation (14), the

Table 1: Distribution and physical parameters of soil layers.

Soil layer	Depth (m)	Water content, (%)	Bulk density (kN/m^3)	Compression modulus (MPa)	Poisson ratio
Sandy silt	1.2	30.9	19.2	5.83	0.3
Silty clay	1.2-1.7	33.9	18.4	3.47	0.3
Clay	1.7-8.9	38.3	18.1	2.62	0.3
Muddy clay	8.9-10.6	48.3	17.2	2.8	0.3
Silty clay	10.6-12.1	35.8	18	3.18	0.3
Silty clay	12.1-26.4	24	19.8	6.97	0.3
Silty clay	26.4-31.4	23.6	19.9	8.23	0.3

Table 2: Measured data of T2 and T4.

Total load (kN)	Settlement (mm)	Load on pile top P_t/(kN)	Uniform load on soil under the cap q_1/(kN/m^2)
T2			
400	2.0	363	17.6
600	2.9	545	25.9
800	4.8	731	32.6
1000	7.0	917	38.9
1200	8.7	1100	47.1
1400	10.4	1284	54.9
1600	14.6	1448	71.5
1800	35.1	1107	326.3
2000	56.9	1258	349.1
T4			
500	1.7	469	15.0
750	2.6	695	25.9
1000	4.3	929	33.6
1250	5.5	1156	44.0
1500	7.4	1381	55.9
1750	9.6	1600	71.0
2000	12.4	1810	89.1
2250	18.0	1978	128.5
2500	49.2	1840	310.8

settlement of the capped pile is calculated:

$$\omega(z) = \frac{P_t \cosh[\lambda(l-z)]}{[k_1 \sinh(\lambda l) + k_2 \cosh(\lambda l)]} + \frac{2q_1}{\pi r E_p}(R-r)\left(\arctan\frac{l}{R-r} - \arctan\frac{z}{R-r}\right). \quad (17)$$

Then substituting Equation (17) into Equation (15), the axial force of the capped pile is calculated:

$$N(z) = \frac{P_t \cdot \cosh[\lambda(l\text{-}z)]}{k_1 \cdot \sinh[\lambda(l-z)] + k_2 \cdot \cosh[\lambda(l-z)]} + 2rq_1\left[(R-r) - z\arctan\frac{R-r}{z}\right]. \quad (18)$$

When $z = 0$, the settlement of the pile top s_t is equal to $\omega(0)$.

$$\omega(0) = s_t = \frac{P_t \cdot \cosh(\lambda l)}{k_1 \cdot \sinh(\lambda l) + k_2 \cdot \cosh(\lambda l)} + \frac{2q_1}{\pi \cdot r \cdot E_p}(R-r)\arctan\frac{l}{R-r}. \quad (19)$$

Equations (18) and (19) are the theoretical expressions of the axial force and the load-settlement curve of a capped pile, respectively. Based on the above analysis, the corresponding computational program is compiled to facilitate the comparison and verification of the calculation results.

3. Comparison and Validation

A case history is introduced to validate the computed results of this method. The Su-Kun-Tai Expressway is located beside Yangcheng Lake in China, and the majority of the route is constructed on a deep, soft, soil foundation. The distribution and physical parameters of the foundation soil layers are shown in Table 1.

Capped piles were used to reduce settlement under the embankment load. The pile body is a PTC-A400-65 concrete pipe pile with lengths of 25 m (T2) and 29 m (T4) in two different test sections. The caps are prefabricated 1.5 m square concrete slabs with thickness of 40 cm. Full-scale tests of capped piles were performed for lateral friction, axial force, and bearing capacity of T2 and T4 piles. The axial force was measured by prefabricated stress gauge at different depths on steel bars in the pile body, and the soil pressure under the pile cap was measured by embedded soil pressure boxes under the pile cap. The bearing capacity of capped piles was determined by load testing [11]. The measured data of the T2 and T4 piles are shown in Table 2 and are used to compare and validate the proposed method.

3.1. Comparison. In order to compare the influence of pile cap on the lateral friction, the capped pile and the ordinary pile are taken into account. The influence of load action on the soil under the pile cap is considered in the lateral friction analysis. The shearing displacement method [35] is adopted for the ordinary pile calculating; the proposed method is adopted for capped pile calculating. The

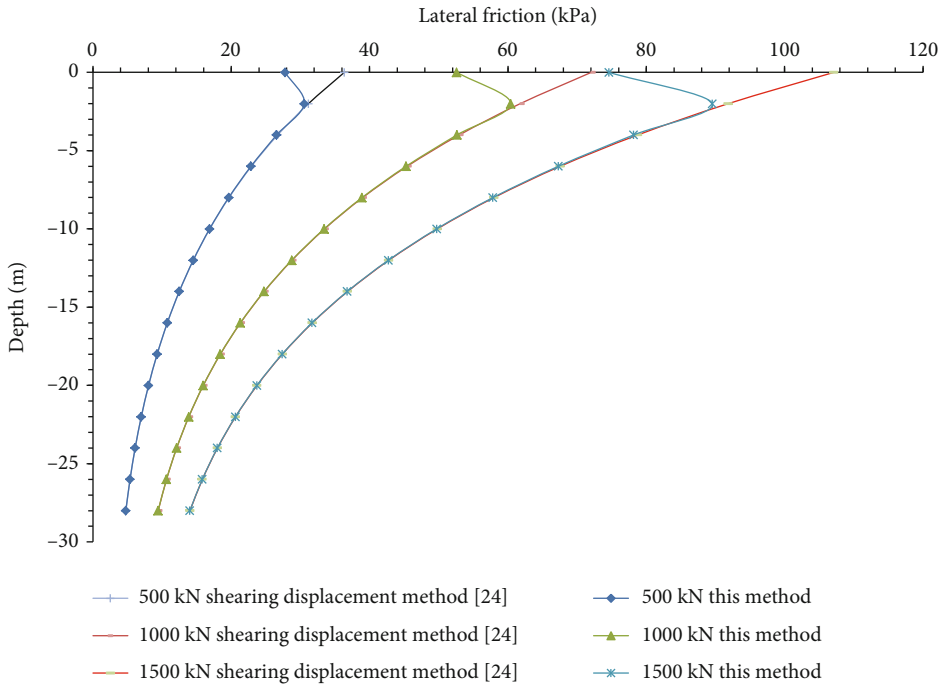

Figure 6: Comparison of lateral friction along pile length of T4.

Table 3: Calculation parameters.

Pile number	Pile length l/(m)	Pile radius r/(m)	Soil deformation modulus E_s/(Mpa)	Pile deformation modulus E_p/(MPa)	Soil shear modulus G_s/(Mpa)	Soil Poisson ratio ν
T2	25	0.2	5.21	30000	2.21	0.3
T4	29	0.2	5.45	30000	2.23	0.3

lateral friction of two types of piles is calculated under the same condition, and the results are shown in Figure 6.

The lateral friction curve of two types of piles in Figure 6 shows obvious difference near the pile top. The lateral friction of capped pile is less than that of ordinary pile. The reason for this phenomenon is that the load on the soil under the pile cap (q_1) reduced the soil deformation, which lead to the pile lateral friction becomes small. The value difference between them is the largest at the pile top and decreases with the depth. This indicates that the load (q_1) affected lateral friction in a certain depth. In this case, the equivalent action radius of q_1 is 0.645 m; the max influenced depth is 2.5 m, which is about 4 times of the load action radius. Beyond this depth, the effect on the lateral friction caused by q_1 is very little and can be ignored. In addition, the load level has a great influence on the lateral friction difference. The higher the load level, the greater the difference. For example, it is 8.5 kPa, 19.5 kPa, and 32.5 kPa when the load level is 500 kN, 1000 kN, and 1500 kN, respectively.

All of the above indicate that when the soil under the pile cap is carrying a load, the lateral friction is affected by the load level and the action radius.

3.2. Validation

3.2.1. Axial Force and Settlement. In order to verify the availability of this method, the calculation results of axial force and the settlement are validated with the measured data. The parameters used in calculation are shown in Table 3.

As seen from Figure 7, the variation of axial force calculated by this method is consistent with the measured data. With the load increasing, the axial force of the pile body increases evenly in most stages. But when the load changes from 2000 kN to 2250 kN, the increase of axial force at the pile tip is smaller. Under the two load levels, the pile body begins to settle faster, and the measured settlement data in Table 2 reflect this phenomenon clearly. This indicates that the soil under the pile tip began to yield and produced plastic deformation, so the axial force increase of pile tip is small. At this time, the load increment of pile body decreased, and the load on soil under the pile cap (q_1) increased correspondingly to balance the total load. When q_1 is increased, the lateral friction near the pile top decreases, leading the axial force to increase. On the whole, the results of axial force computed by this method are consistent with the experimental phenomenon and the theoretical analysis.

The calculated load-settlement curves (Figure 8) are as follow:

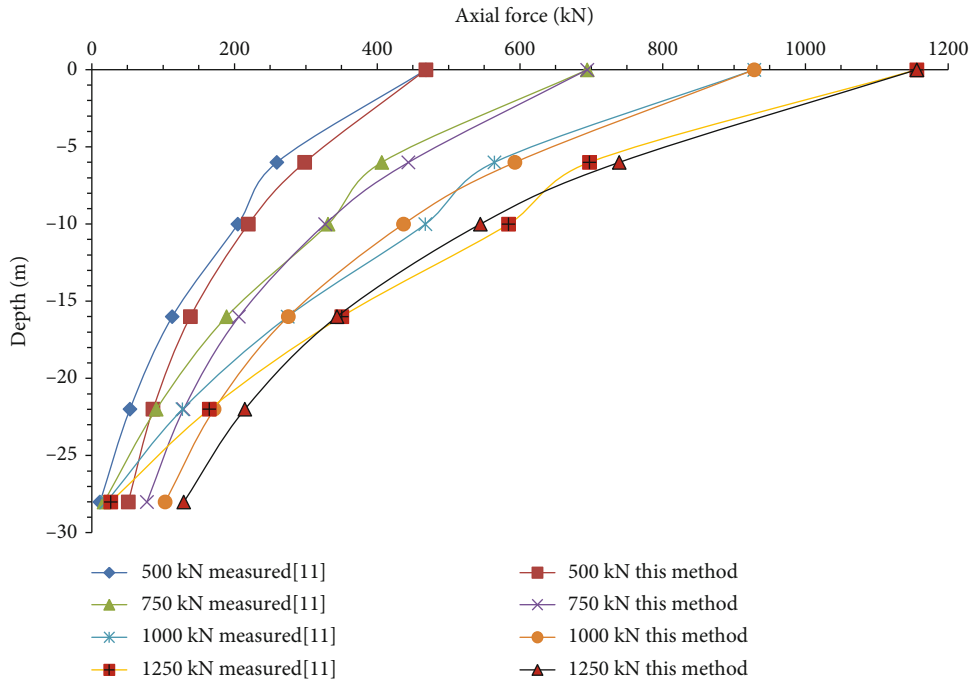

(a) Load 500kN-1250kN

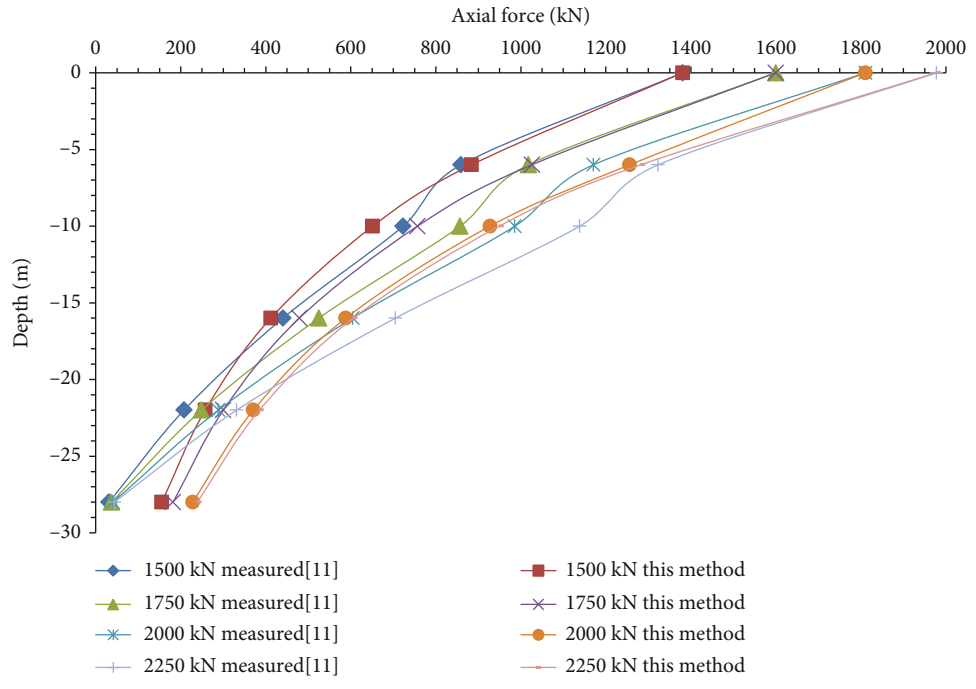

(b) Load 1500kN-2000kN

Figure 7: Axial force curves of T4 along pile length.

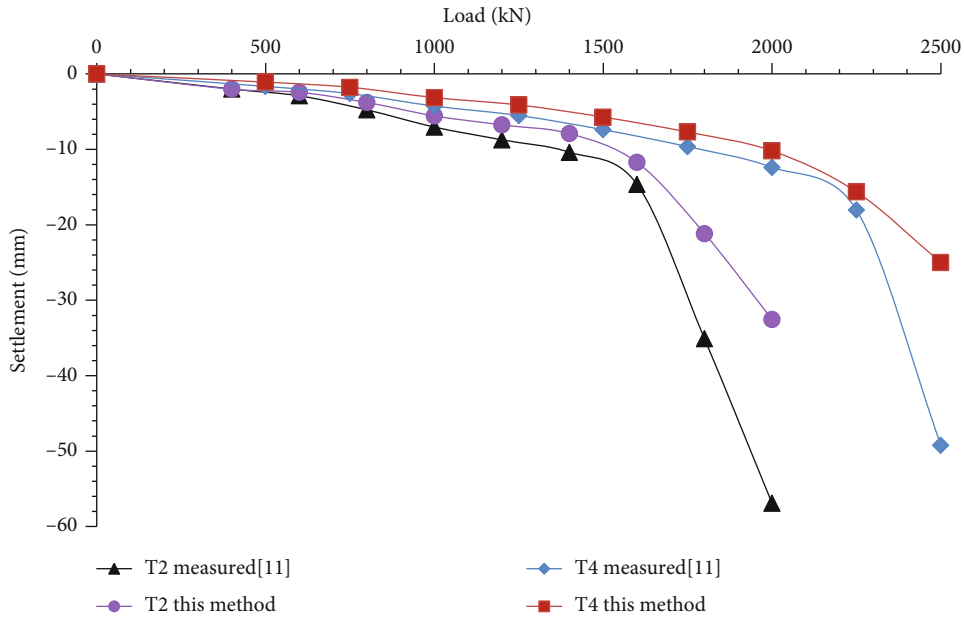

Figure 8: Load-settlement curves of T2 and T4.

Figure 8 demonstrates that the variation of load-settlement curves computed by this method is consistent with that of the measured curves, but the calculated settlements are slightly less than the measured data. In the two cases (T2 and T4), the error of settlement increases when the soil is close to failure. The reason for this phenomenon is that when the capped pile is approaching the ultimate load, the differential displacement between pile and soil is increased gradually, the condition of equal strain cannot be strictly satisfied, which leads to a larger error.

4. Conclusions

Compared with the ordinary pile, the pile–soil interaction of capped pile is more complicated. In this study, we proposed an analysis method of pile–soil interaction for capped piles considering the load action of the soil under the pile cap. We established an analysis model of pile–soil interaction according to the mechanical characteristics of capped piles and analyzed the lateral friction by combining the shearing displacement method and Boussinesq solutions. Theoretical analytical expressions of lateral friction, axial force, and load-settlement curves were obtained by establishing the equilibrium differential equation of a pile body and solving it. By comparing the variation of lateral friction curve between ordinary pile and capped pile, it is found that the load acting on the soil under the cap reduces the lateral friction value in a depth of about 4 times the load action radius. Beyond this depth, the influence can be ignored. This is unfavorable to the bearing capacity of pile body; for short piles with large pile caps, this phenomenon should be fully considered in design. The axial force and load-settlement curves calculated by this method are validated by a case history of reinforcing subgrade with capped piles. The result shows that the variations of axial forces agree with the experimental date and theoretical analysis and the variation of load-settlement curves are consistent with that of the measured curves. The error of load-settlement increases when the soil is close to failure, which need to be further studied.

Data Availability

Yes, we checked it carefully and comfirmed that all data, models and code generated at the manuscript could be obtained from the corresponding author.

Conflicts of Interest

The authors declare that they have no conflicts of interest.

Authors' Contributions

Shilin Luo conceptualized the study and was responsible for the methodology and revision. Mingquan Liu was responsible for the algorithms and analysis and wrote the original draft. Jianqing Jiang and Ailifeila Aierken were responsible for the data curation and language editing. Jin Chang was responsible for the revision. Xuewen Zhang and Rui Zhang were responsible for the software and validation.

Acknowledgments

This work was supported by the National Natural Science Foundation of China (42107166), Hunan Provincial Natural Science Foundation (Nos 22021JJ40632 and 2021JJ30758), and Scientific Research Project from the Education Department of Hunan Province (Nos 21C0753 and 21C0740). We also thank Dr. Yan-lin Zhao for his help in the improvement of the text's language.

References

[1] W. P. Hong and S. Hong, "Piled embankment to prevent damage to pipe buried in soft grounds undergoing lateral flow," *Marine Georesources & Geotechnology*, vol. 35, no. 5, pp. 719–729, 2016.

[2] S. Rezaeimalek, N. Abdolreza, J. Huang, S. Bin-Shafique, and S. T. Gilazghi, "Comparison of short-term and long-term performances for polymer-stabilized sand and clay," *Journal of Traffic and Transportation Engineering (English Edition)*, vol. 4, no. 2, pp. 145–155, 2017.

[3] M. A. Nunez, L. Briançon, and D. Dias, "Analyses of a pile-supported embankment over soft clay: full-scale experiment, analytical and numerical approaches," *Engineering Geology*, vol. 153, pp. 53–67, 2013.

[4] L. Jinbo, Y. Kang, Z. Xing, Y. Jinyou, and W. Menghua, "Experimental study on pile-soil stress ratio of the composite foundation of pipe-pile with cap and holes," *Chinese Journal of Rock Mechanics and Engineering.*, vol. 36, no. s1, pp. 3607–3617, 2017.

[5] W. Z. Liu, J. H. Zhang, and H. Zhang, "Analysis on pile-soil stress ratio of composite foundation with sparse capped-piles under lime-soil embankment load," *Applied Mechanics and Materials*, vol. 501-504, pp. 124–131, 2014.

[6] X. M. Lou, G. B. Jiang, and H. Y. Xu, "Analysis on load transfer for single pile composite foundation under embankments based on elastic theory," *Ground Improvement and Geosynthetics*, pp. 187–196, 2010.

[7] Y. K. Chow, "Pile-cap-pile-group interaction in nonhomogeneous soil," *International Journal of Rock Mechanics and Mining Sciences & Geomechanics*, vol. 29, no. 3, p. A184, 1992.

[8] C. C. Mendoza, B. Caicedo, and R. Cunha, "Determination of vertical bearing capacity of pile foundation systems in tropical soils with uncertain and highly variable properties," *Journal of Performance of Constructed Facilities*, vol. 31, no. 1, p. 04016068, 2017.

[9] D. Dia and J. Grippon, "Numerical modelling of a pile-supported embankment using variable inertia piles," *Structural Engineering and Mechanics*, vol. 61, no. 2, pp. 245–253, 2017.

[10] Y. Sang, Z. Wang, S. Yu, and H. Zhao, "The loading test on the singe pile with pile cap in transparent soil model," *Geotechnical Testing Journal*, vol. 42, no. 2, pp. 385–406, 2019.

[11] L. Jin-bo and C. Cong-xin, "In-situ prototype test study of composite foundation of rigid pile with cap," *Chinese Journal of Rock Mechanics and Engineering*, vol. 29, no. 8, pp. 1713–1720, 2010.

[12] N. Borthakur and A. K. Dey, "Experimental investigation on load carrying capacity of micropiles in soft clay," *Arabian Journal for Science and Engineering*, vol. 43, no. 4, pp. 1969–1981, 2018.

[13] B. Le Hello and P. Villard, "Embankments reinforced by piles and geosynthetics- numerical and experimental studies dealing with the transfer of load on the soil embankment," *Engineering Geology*, vol. 106, no. 1-2, pp. 78–91, 2009.

[14] M. Moreno, R. Maia, and L. Couto, "Effects of relative column width and pile-cap elevation on local scour depth around complex piers," *Journal of Hydraulic Engineering*, vol. 142, no. 2, p. 04015051, 2016.

[15] Y. Zhao, C. L. Wang, and J. Bi, "Analysis of fractured rock permeability evolution under unloading conditions by the model of elastoplastic contact between rough surfaces," *Rock Mechanics and Rock Engineering*, vol. 53, no. 12, pp. 5795–5808, 2020.

[16] Y. Zhao, C. L. Wang, J. Q. Yang, and J. Bi, "Coupling model of groundwater and land subsidence and simulation of emergency water supply in Ningbo urban Area, China," *Journal of Hydrology*, vol. 594, article 125956, 2021.

[17] Y. Zhao, J. Bi, C. L. Wang, and P. F. Liu, "Effect of unloading rate on the mechanical behavior and fracture characteristics of sandstones under complex triaxial stress conditions," *Rock Mechanics and Rock Engineering*, vol. 54, no. 9, pp. 4851–4866, 2021.

[18] Y. Zhao, C. L. Wang, L. Ning, H. F. Zhao, and J. Bi, "Pore and fracture development in coal under stress conditions based on nuclear magnetic resonance and fractal theory," *Fuel*, vol. 309, article 122112, 2022.

[19] Y. Zhao, C. Wang, M. Teng, and J. Bi, "Observation on microstructure and shear behavior of mortar due to thermal shock," *Cement and Concrete Composites*, vol. 121, article 104106, 2021.

[20] W. Liu and M. Novak, "Soil–pile–cap static interaction analysis by finite and infinite elements," *Canadian Geotechnical Journal*, vol. 28, no. 6, pp. 771–783, 1991.

[21] R. K. Rowe and K. W. Liu, "Three-dimensional finite element modelling of a full-scale geosynthetic -reinforced, pile-supported embankment," *Canadian Geotechnical Journal.*, vol. 52, no. 12, pp. 2041–2054, 2015.

[22] X. Tan, M. Zhao, and W. Chen, "Numerical simulation of a single stone column in soft clay using the discrete-element method," *International Journal of Geomechanics*, vol. 18, no. 12, p. 04018176, 2018.

[23] Q. Fu, H. Liu, X. Ding, and C. Zheng, "Numerical investigation of piled raft foundation in mitigating embankment vibrations induced by high-speed trains," *Journal of Central South University*, vol. 22, no. 11, pp. 4434–4444, 2015.

[24] Y. Zhao, Y. Zhang, H. Yang, Q. Liu, and G. Tian, "Experimental study on relationship between fracture propagation and pumping parameters under constant pressure injection conditions," *Fuel*, vol. 307, p. 121789, 2022.

[25] J. T. Yi, F. Liu, T. B. Zhang, K. Yao, and G. Zhen, "A large deformation finite element investigation of pile group installations with consideration of intervening consolidation," *Applied Ocean research*, vol. 112, article 102698, 2021.

[26] F. Liu, J. Yi, and P. Cheng, "Numerical simulation of set-up around shaft of XCC pile in clay," *Geomechanics and Engineering*, vol. 21, no. 5, pp. 489–501, 2020.

[27] Y. Peng, X. Ding, Y. Xiao, X. Deng, and W. Deng, "Detailed amount of particle breakage in non-uniformly graded sands under one-dimensional compression," *Canadian Geotechnical Journal*, vol. 57, no. 8, pp. 1239–1246, 2020.

[28] Y. Peng, H. Liu, C. Li, X. Ding, X. Deng, and C. Wang, "The detailed particle breakage around the pile in coral sand," *Acta Geotechnica*, vol. 16, no. 6, pp. 1971–1981, 2021.

[29] Y. Peng, X. Ding, Y. Xiao, J. Chu, and W. Deng, "Study of particle breakage behaviour of calcareous sand by dyeing tracking and particle image segmentation method," *Rock and Soil Mechanics*, vol. 40, no. 7, pp. 2663–2672, 2019.

[30] S. P. Shang, Y. X. Du, and F. Zhou, "Study on the interaction of subsoil and piled box (raft) foundation," *China Civ. Eng.*, vol. 34, no. 4, pp. 93–97, 2001.

[31] W. Cui and X. Zheng, "Analysis of the response of pile groups considering pile–cap–soil interaction in layered soil," *Soil Mechanics and Foundation Engineering*, vol. 55, no. 2, pp. 87–95, 2018.

[32] L. Jin-bo and C. Cong-xin, "Research on load transfer mechanism of composite foundation of rigid pile with cap based on hyperbolic model," *Rock and Soil Mechanics*, vol. 30, no. 11, pp. 3385–3391, 2010.

[33] Z. F. Wang, W. C. Cheng, Y. Q. Wang, and J. Q. Du, "Simple method to predict settlement of composite foundation under embankment," *International Journal of Geomechanics*, vol. 18, no. 12, p. 04018158, 2018.

[34] C. Chang-Fu, Z. Xiang-Long, and W. Yan-Quan, "Load-displacement relation- ship of short stiff piles with big cap based on block displacement method," *Rock and Soil Mechanics*, vol. 38, no. 12, 2017.

[35] M. F. Rondoloph and C. P. Worth, "Analysis of deformation of vertically loaded piles," *Journal of the Geotechnical Engineering Division*, vol. 104, no. 12, pp. 1465–1488, 1978.

[36] J. Boussinesq, *Application des potentiels a l'etude de l'equilibre et du mouvement des solides elastiques*, Gauthier-Villars, Paris, 1885.